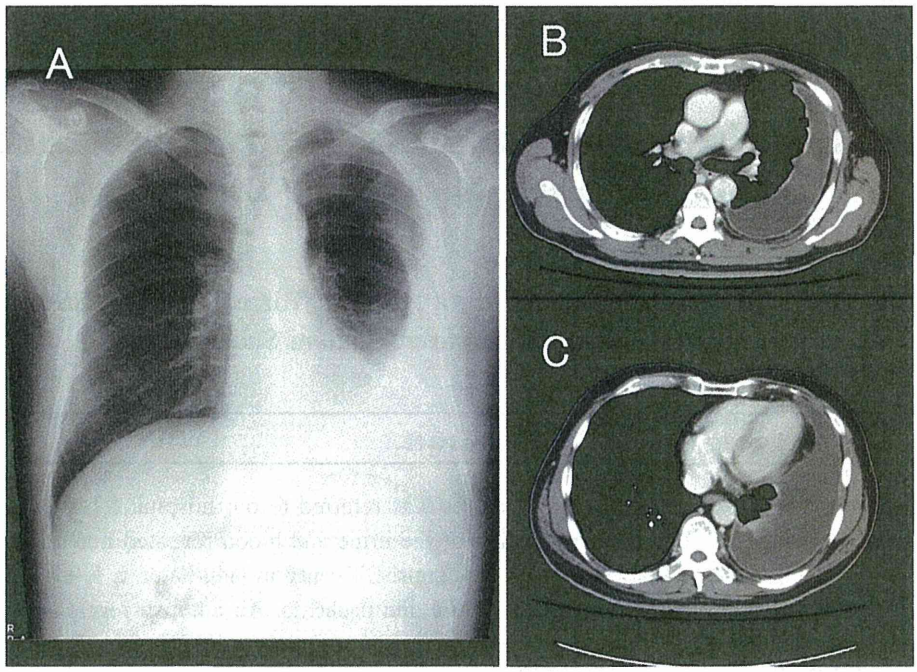

Figure 1. **Chest radiography (A) and computed tomography of the chest (B, C) performed on the first admission showing left massive pleural effusion. No pleural tumors, pulmonary nodules or hilar or mediastinal lymphadenopathy are evident.**

were obtained for urinary light-chain excretion. Radiography and computed tomography of the chest showed left massive effusion (Fig. 1A-C). The pleural fluid contained cloudy exudate with an elevated level of hyaluronic acid (171,000 ng/mL) and no malignant cells. No microorganisms were detected in the pleural fluid. A thoracoscopic examination was performed under suspicion of malignant pleural mesothelioma. However, a macroscopic examination of the left thorax revealed no abnormalities, and a pleural biopsy did not yield a definitive diagnosis. The patient declined further examinations due to his impaired performance status resulting from multiple brain infarctions and dementia. After undergoing pleurodesis, he was followed up with supportive care as well as the prescription of a diuretic and anticoagulant for nephrotic syndrome by a local general physician. The edema persisted without any thrombosis. However, the patient began to complain of left chest pain and loss of appetite 20 months later and was again referred to our hospital. Radiography and computed tomography of the chest revealed a left pleural tumor, and computed tomography of the abdomen demonstrated left adrenal metastasis and peritoneal dissemination (Fig. 2A-C). The laboratory data disclosed positive urine protein (3.7 g/day) with normal urine sediment, hypoproteinemia (serum total protein, 5.6 g/dL), hypoalbuminemia (serum albumin, 1.3 g/dL) and mild dehydration (blood urea nitrogen, 29 mg/dL; serum creatinine, 1.1 mg/dL). Palliative treatment was administered due to the patient's rapidly worsening respiratory and general condition. He died of respiratory failure and cachexia on hospital day 11.

An autopsy revealed a left pleural tumor that had metastasized to the lung parenchyma, hilar lymph nodes, liver, left adrenal gland, multiple bones and peritoneum. A microscopic examination of the pleural tumor showed epithelioid tumor cells (Fig. 3A) that were immunohistochemically positive for calretinin, D2-40 and cytokeratin (CK) 5/6 (Fig. 3B-D) and negative for carcinoembryonic antigen and thyroid transcription factor 1. Immunohistochemical staining confirmed the diagnosis of epithelioid pleural mesothelioma. Light microscopic findings of the glomeruli and uriniferous tubules were normal. Taken together with the laboratory findings, a diagnosis of minimal-change nephrotic syndrome was considered, although no electron microscopic studies were performed.

Discussion

Malignant mesothelioma cells are potent sources of various cytokines, some of which are involved in the aggressive growth and spread of malignant mesothelioma. These cytokines are also thought to be involved in various paraneoplastic syndromes, including immunosuppression, thrombocytosis, amyloidosis and hypoglycemia (2).

In the present case, whether malignant mesothelioma was involved in the development of nephrotic syndrome remains unclear. However, a review of the English literature identified seven reported cases of malignant mesothelioma associated with nephrotic syndrome (3-9). Among these seven cases, the primary site of mesothelioma was the pleura in five cases, peritoneum in one case and tunica vaginalis testis in one case. The histological type in the five reported cases of pleural mesothelioma was epithelioid in three cases, sar-

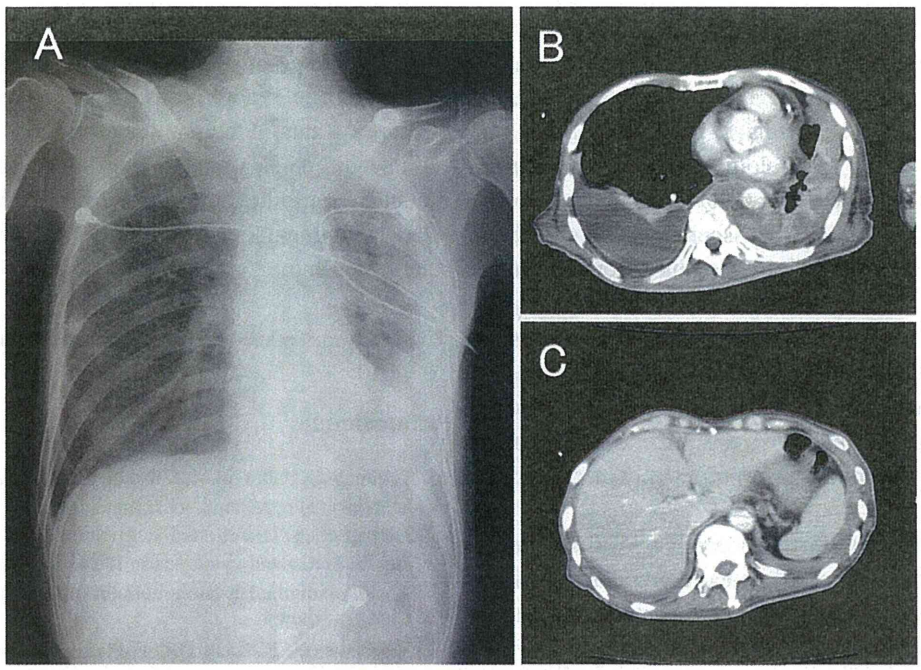

Figure 2. **Chest radiography (A) and computed tomography of the chest (B) and abdomen (C) performed on the second admission showing a left pleural tumor, right pleural effusion (likely due to nephrotic syndrome), ascites and left adrenal metastasis.**

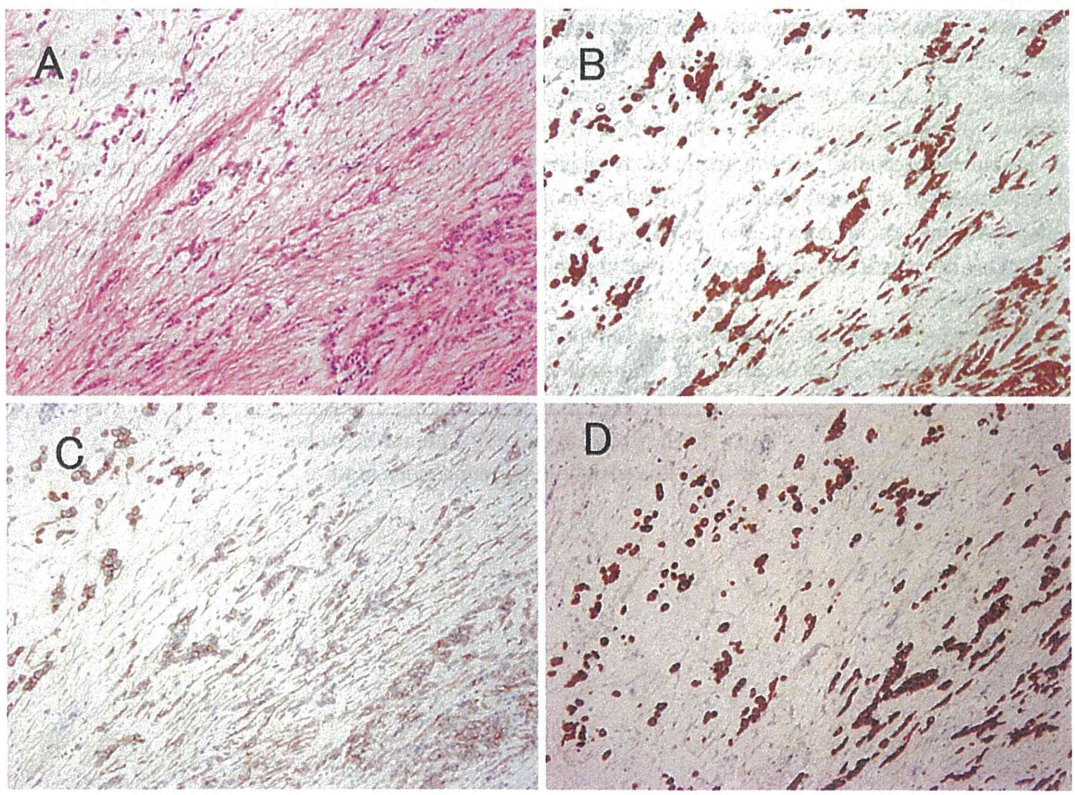

Figure 3. **Autopsy specimen of the pleural tumor showing epithelioid mesothelioma cells (A, Hematoxylin and Eosin staining, 200×) that are immunohistochemically positive for calretinin (B), D2-40 (C) and CK5/6 (D).**

comatoid in one case and not described in the remaining case. The histological type in the reported cases of peritoneal mesothelioma and mesothelioma of the tunica vaginalis testes was epithelioid. The histological findings of the glomeruli showed minimal changes in three of the seven cases, membranous nephropathy in two cases and mesangial proliferative glomerulonephritis in one case, with no examinations performed in the remaining case. The temporal asso-

ciation between malignant mesothelioma and nephrotic syndrome was concurrent in six of the seven cases, with malignant mesothelioma preceding the onset of minimal-change nephrotic syndrome by 11 months in one case. Solid tumors, such as lung cancer and colon cancer, are considered to be responsible for 5-10% of cases of membranous nephropathy in adults (9). Malignancy associated with membranous nephropathy may occur 12-18 months before, simultaneously with or 12-18 months after the manifestations of membranous glomerulopathy first appear (6). In the present case, malignant pleural mesothelioma became apparent and was diagnosed 20 months after the initial presentation. However, we believe that our patient had subclinical malignant mesothelioma that was not macroscopically detectable on the initial presentation.

Tumor antigens are presumably deposited in the glomeruli, followed by antibody deposition and complement activation, thus leading to epithelial cell and basement membrane injury and proteinuria due to the associated increase in glomerular permeability (6). In contrast with paraneoplastic membranous nephropathy, minimal-change glomerular disease is the most common glomerulopathy associated with lymphoproliferative malignancies, such as Hodgkin's disease, and is thought to be a disorder of the T-cell function (3). Lymphocytes obtained from patients with minimal-change nephrotic syndrome yield cytokines that can increase capillary permeability (10). Based on these previous reports, we speculate that malignant mesothelioma cell-derived cytokines, such as vascular endothelial growth factor, may play a role in the development of minimal-change nephrotic syndrome in patients with malignant mesothelioma. To clarify this hypothesis, further investigations involving a large number of patients are needed.

In conclusion, we herein reported an autopsy case of malignant pleural mesothelioma associated with minimal-change nephrotic syndrome. We were able to observe the natural course of malignant pleural mesothelioma associated with nephrotic syndrome due to the patient's impaired performance status. A review of the English literature on nephrotic syndrome as a paraneoplastic syndrome associated with malignant mesothelioma suggested a possible correlation between malignant mesothelioma and minimal-change nephrotic syndrome.

The authors state that they have no Conflict of Interest (COI).

References

1. Yeung SC, Habra MA, Thosani SM. Lung cancer-induced paraneoplastic syndrome. Curr Opin Pulm Med **17**: 260-268, 2011.
2. Fitzpatrick DR, Peroni DJ, Bielefeldt-Ohmann H. The role of growth factor and cytokines in the tumorigenesis and immunobiology of malignant mesothelioma. Am J Respir Cell Mol Biol **12**: 455-460, 1995.
3. Schroeter NJ, Rushing DA, Parker JP, Beltaos E. Minimal-change nephrotic syndrome associate with malignant mesothelioma. Arch Intern Med **14**: 1834-1866, 1986.
4. Tanaka S, Oda H, Satta H, et al. Nephrotic syndrome associated with malignant mesothelioma. Nephron **67**: 510-511, 1994.
5. Galesic K, Bozic B, Heinzl R, Scukanec-Spoljar M, Bozikov V. Pleural mesothelioma and membranous nephropathy. Nephron **84**: 71-74, 2000.
6. Farmer CK, Goldsmith DJ. Nephrotic syndrome and mesenteric infarction secondary to metastatic mesothelioma. Postgrad Med J **77**: 333-334, 2001.
7. Bacchetta J, Ranchère D, Dijoud F, Droz JP. Mesothelioma of the testis and nephrotic syndrome: a case report. J Med Case Rep **3**: 7248, 2009.
8. Dogan M, Ozal G, Savas B, et al. Malign peritoneal mesothelioma with nephrotic syndrome. Bratisl Lek Listy **113**: 43-45, 2012.
9. Burstein DM, Korbet SM, Schwartz MM. Membranous glomerulonephritis and Malignancy. Am J Kidney Dis **22**: 5-10, 1993.
10. Jaurand MC, Fleury-Feith J. Pathogenesis of malignant pleural mesothelioma. Respirology **10**: 2-8, 2005.

Pathology – Research and Practice xxx (2013) xxx–xxx

Contents lists available at ScienceDirect

Pathology – Research and Practice

journal homepage: www.elsevier.com/locate/prp

Teaching Case

Breakages at YWHAE, FAM22A, and FAM22B loci in uterine angiosarcoma: A case report with immunohistochemical and genetic analysis

Shioto Suzuki [a,*], Fumihiko Tanioka [a], Hiroshi Minato [b], Ayse Ayhan [c], Masako Kasami [d], Haruhiko Sugimura [e]

[a] Division of Pathology, Iwata City Hospital, Japan
[b] Department of Pathology and Laboratory Medicine, Kanazawa Medical University, Japan
[c] Department of Pathology, Seirei Mikatahara General Hospital, Japan
[d] Division of Laboratory Medicine, Iwata City Hospital, Japan
[e] Department of Tumor Pathology, Hamamatsu University School of Medicine, Japan

ARTICLE INFO

Article history:
Received 22 April 2013
Received in revised form 9 September 2013
Accepted 9 September 2013

Keywords:
Angiosarcoma
Uterus
YWHAE
FAM22

ABSTRACT

Described herein is the first reported case of a uterine angiosarcoma with breakages at three loci, YWHAE (17p13), FAM22A (10q23) and FAM22B (10q22). A 62-year-old postmenopausal woman was found to have endometrial thickening of her uterus. An endometrial biopsy indicated a malignant, spindle cell neoplasm. A total hysterectomy with bilateral salpingooophorectomy was performed. Histologic examination of the uterine specimen showed a malignant tumor consisting of irregular rudimentary vascular channels and solid small nests diffusely infiltrating to the middle of the myometrial wall. The tumor cells were epithelioid, and displayed eosinophilic cytoplasm and vesicular nuclei in some areas of the tumor. Immunohistochemically, the tumor cells showed vascular differentiation; they were diffusely positive for CD31 and D2-40 but were negative for factor VIII and CD34. In the course of the procedure of differential diagnoses, we included fluorescence *in situ* hybridization analysis for detection of a FAM22B-YWHAE fusion gene resulting from t(10;17)(q22;p13), recently reported in a series of endometrial stromal sarcoma, and unexpectedly identified breakages at three loci, *i.e.* YWHAE (17p13), FAM22A (10q23) and FAM22B (10q22). Collectively, these findings suggest that abnormality in the loci of YWHAE, FAM22A and FAM22B, which are known to be associated with oncogenesis of endometrial stromal sarcoma, may contribute to the development of uterine angiosarcoma.

Introduction

Uterine sarcomas other than leiomyosarcomas and endometrial stromal sarcomas (ESS) are uncommon [1,12]. In particular, uterine angiosarcoma is very rare, and fewer than 20 cases with sufficient immunohistochemical or electron microscopy findings have been reported in the medical literature over the past 20 years [3,4,10,12,13,17]. Most patients were postmenopausal and generally presented with heavy uterine bleeding, weight loss, and a pelvic mass [3,12,13]. Uterine angiosarcomas are usually highly aggressive and extend beyond the uterus, sometimes recurring within weeks to months after the initial diagnosis [3,12,13]. Unfortunately, the oncogenesis of uterine angiosarcomas is unknown.

Tumor is caused by accumulation of genomic abnormalities, including single-nucleotide variations, copy number changes and fusion genes [8,11,14,21]. Thus, their detection is of critical importance for fully understanding oncogenesis, improvement of diagnosis, as well as the development of novel therapeutics. Unfortunately, compared with hematological disorders, our knowledge of the karyotypic features of solid tumors is fragmentary at best. All solid tumors, benign and malignant, account for only 27% of the total number of cases with an abnormal karyotype reported in the literature [11]. However, to date, new technologies, including second-generation sequencer, have been shown to provide powerful methods to detect genomic abnormalities [21], and have confirmed that recurrent fusion genes characterize significant subsets of sarcomas [8,11]. For example, a YWHAE-FAM22 fusion gene resulting from t(10;17)(q22;p13) was recently reported in a series of ESS [6–8]. During evolving this surveillance, we checked this fusion gene in the series of uterine mesenchymal tumors, including not only ESS but also others (data not shown). To date, contributory molecular alterations for uterine angiosarcomas have

* Corresponding author at: Division of Pathology, Iwata City Hospital, 512-3 Ookubo, Iwata, Shizuoka 438-8550, Japan. Tel.: +81 538 38 5000.
E-mail address: shiosuzuki-path@umin.net (S. Suzuki).

0344-0338/$ – see front matter © 2013 Elsevier GmbH. All rights reserved.
http://dx.doi.org/10.1016/j.prp.2013.09.009

not been reported. In this article, we describe the first reported case of uterine angiosarcoma with breakages at three loci, *i.e.* YWHAE (17p13), FAM22A (10q23) and FAM22B (10q22), which is serendipitously encountered in the procedure of extended surveillance for uterine mesenchymal tumors.

Clinical summary

A 62-year-old postmenopausal woman sought medical advice because of uterine bleeding. A pelvic ultrasound revealed endometrial thickening (1.02 cm). An endometrial biopsy was positive for a malignant, epithelioid cell neoplasm. A computed tomography (CT) scan and magnetic resonance imaging examination performed at the time of hospitalization revealed a mass in the posterior wall of the uterus and no other mass lesion. A total hysterectomy with bilateral salpingooophorectomy was performed.

Materials and methods

Histopathologic and immunohistochemical examination

All the tissues were fixed in 10% buffered formalin and embedded in paraffin after routine processing, sectioning, and staining with hematoxylin and eosin (H&E). Immunostaining was performed using antibodies for the following antigens: bcl-2 (DAKO, Glostrup, Denmark), CD10 (Leica Biosystems, Newcastle, United Kingdom), caldesmon (DAKO), calponin (DAKO), CD31 (DAKO), CD34 class II (DAKO), cyclinD1 (Nichirei, Tokyo, Japan), cytokeratin AE1/AE3 (DAKO), D2-40 (DAKO), epithelial membrane antigen (EMA, DAKO), estrogen receptor (ER, DAKO), factor VIII (DAKO), HMB45 (DAKO), MIB-1 (DAKO), p53 (DAKO), progesterone receptor (PgR, DAKO), S-100 (DAKO), and smooth muscle actin (SMA, DAKO).

Fluorescence in situ hybridization (FISH) analysis

According to the protocol of a previous study [7], FISH probes flanking genes of interest (YWHAE, FAM22A, and FAM22B) were prepared from the Bacterial Artificial Chromosome (BAC) library. The FISH procedure was performed as previously reported [19,20]. BAC probes flanking FAM22A (RP11-52G13 and RP11-57C13), another BAC probe located in the FAM22B locus (RP11-31L4, RP11-131C15 and RP11-119F19), and a BAC probe in YWHAE (RP11-22G12, RP11-961A15 and RP11-818O24) were purchased from Advanced GenoTechs Co. (Tsukuba). The chromosomal positions of the probes are shown in Fig. 1. All the probes were confirmed to be correct by hybridizing them to a metaphase human chromosome spread (data not shown). To detect the breakages of FAM22A, FAM22B and YWHAE loci, RP11-52G13 and RP11-57C13, RP11-31L4 and RP11-131C15, and RP11-22G12 and RP11-961A15 were used, respectively. To identify the breakages of FAM22A, FAM22B and YWHAE loci, RP11-52G13, RP11-31L4 and RP11-22G12 probes were nick-translated using Orange dUTP (2N33-50; Abbot, IL, USA), while RP11-57C13, RP11-131C15 and RP11-961A15 were nick-translated using Green dUTP (2N32-50; Abbot, IL). To identify the fusion signals, the combinations of RP11-52G13, RP11-57C13, and RP11-818O24 were used to detect the fusion of FAM22A and YWHAE, and a combination of RP11-119F19 and RP11-818O24 was used to detect the fusion of FAM22B and YWHAE. To detect fusion, both the FAM22A and FAM22B probes were nick-translated using Orange dUTP (2N33-50), while the YWHAE probe was nick-translated using Green dUTP (2N32-50). The nuclei were stained with 4,6-diamino-2-phenyl indole dihydrochloride (DAPI, Abbot).

Hybridization was performed on 4-μm-thick sections using a standard pretreatment and hybridization protocol. The slides were reviewed manually with at least 50 tumor nuclei evaluated for each case. The cutoff value of >10% *ca.* in tumor cell nuclei showing a split signal was considered positive for the rearrangement of the flanked gene. This cut off value of FISH analyses for a fusion gene-positive case was much safer in the light of our previous report [16], where amplifications were evaluated and the false positive rate may be higher, that is, split signals in the non-tumor epithelial, mesenchymal or lymphocytic cells were almost negligible in this study.

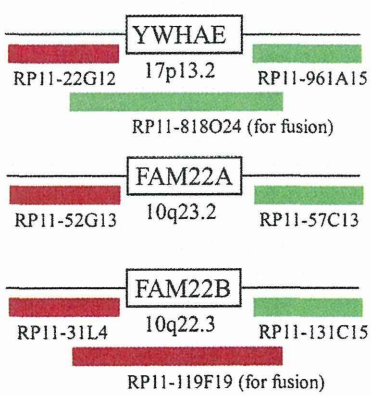

Fig. 1. The chromosomal positions of FISH probes flanking genes of interest (YWHAE, FAM22A, and FAM22B).

Results

Pathologic findings in the uterus

The uterus weighed 140 g and measured 7.5 cm × 5.5 cm × 3.5 cm. The uterus contained an ill-circumscribed endometrial tan-gray mass measuring 3.0 cm at its largest dimension; another additional 4 nodules were found in the myometrium (Fig. 2a). The cervix and adnexa were unremarkable.

Histologic examination of the uterine specimen showed an endometrial malignant tumor diffusely infiltrating the endometrium, and this tumor invaded the half thickness of the myometrium (Fig. 2b); the tumor had an irregular vasoformative structure (Fig. 2c), not showing angiocentric pattern, one of the typical findings of epithelioid hemangioendothelioma; the tumor also contained solid small nests (Fig. 2d). The tumor cells were epithelioid, and sometimes exhibited eosinophilic cytoplasm and vesicular nuclei with intense cellular atypia (Fig. 2d). Frequent mitotic figures were not observed. The tumor was distinct from the 4 coincidental leiomyomas found in the myometrium. No microscopic evidence of neoplastic infiltration of the cervix, fallopian tubes, or ovaries was seen.

Immunohistochemical examination

Immunohistochemically, the tumor cells were diffusely positive for CD31 (Fig. 3a), D2-40, and bcl-2, and were focally positive for p53 and cyclin D1 (Fig. 3b); the tumor cells were negative for CD10 (Fig. 3c), ER, PgR, CD34, factor VIII, cytokeratin AE1/AE3, EMA, SMA, caldesmon, calponin, S-100, and HMB45. Positive staining for MIB-1 was observed in 3% of the tumor cells. Based on the histologic and immunohistochemical findings, the tumor was diagnosed as a uterine angiosarcoma.

Please cite this article in press as: S. Suzuki, et al., Breakages at YWHAE, FAM22A, and FAM22B loci in uterine angiosarcoma: A case report with immunohistochemical and genetic analysis, Pathol. – Res. Pract (2013), http://dx.doi.org/10.1016/j.prp.2013.09.009

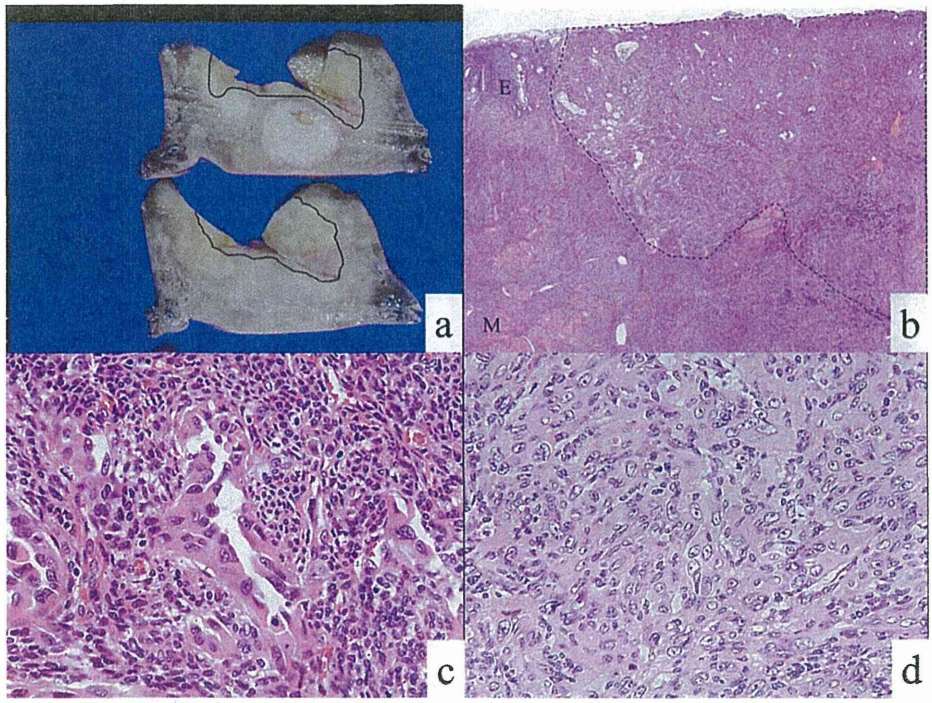

Fig. 2. Pathological findings of the uterine angiosarcoma. (a) Cross-sections show an ill-circumscribed endometrial tan-gray mass (enclosed by curved line) and nodules in the myometrium. (b–d) The tumor (enclosed by broken line) arises from the endometrium (E) and invades myometrium (M) (b), forming irregular rudimentary vascular channels (c) and small solid nests (d). The tumor cells are epithelioid and sometimes exhibited vesicular nuclei with intense cellular atypia (d).

FISH analysis

The two probes at the locations flanking the FAM22A, FAM22B, and YWHAE locus were shown as separate signals with a distance of 3 or more dot sizes (Fig. 4a–c). These results demonstrated that breakages of the YWHAE, FAM22A, and FAM22B loci had been generated in the tumor cells. A single yellow (overlapping) signal, including an orange (FAM22A) and green (YWHAE) signal, was not

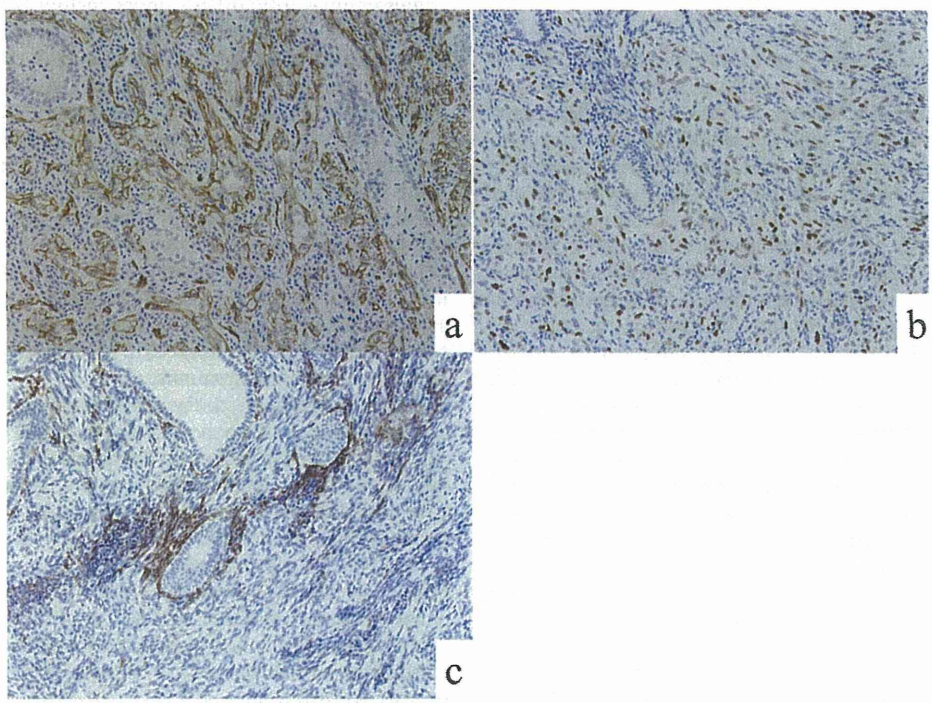

Fig. 3. Immunohistochemical findings of the uterine angiosarcoma. (a) The tumor cells show CD31 immunoreactivity. (b) The tumor cells are focally positive for cyclin D1. (c) CD10 staining is visible only in the residual narrow space around the endometrial gland and not in the infiltrating tumor cells.

Please cite this article in press as: S. Suzuki, et al., Breakages at YWHAE, FAM22A, and FAM22B loci in uterine angiosarcoma: A case report with immunohistochemical and genetic analysis, Pathol. – Res. Pract (2013), http://dx.doi.org/10.1016/j.prp.2013.09.009

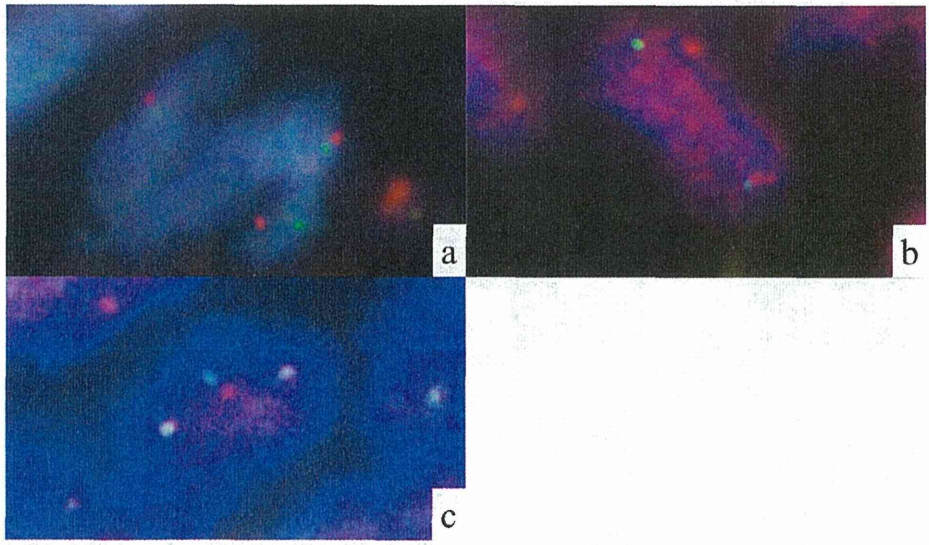

Fig. 4. Representative findings of the uterine angiosarcoma by FISH. (a–c) The two probes at the locations flanking the FAM22A locus (a), FAM22B locus (b) and YWHAE locus (c) are shown as separate signals (green and orange). (For interpretation of the references to color in this figure legend, the reader is referred to the web version of this article.)

clearly shown in tumor cells exhibiting prominent nuclear atypia, whereas FAM22B-YWHAE fusion signal was not observed either (data not shown).

Treatment and follow up

She was alive and well 50 months after surgery. CT scan confirmed multiple small nodules in bilateral lungs and a small amount of right pleural effusion. Excisional biopsy of pleura was positive for metastatic angiosarcoma. She has been given adjuvant chemotherapy.

Discussion

Uterine angiosarcoma is very rare as compared with ESS or leiomyosarcoma [1,12]. Microscopically, angiosarcoma contains incomplete vascular channels lined by atypical cuboidal cells and solid areas with atypical epithelioid cells that exhibit eosinophilic cytoplasm and round nuclei, and does not show the angiocentric pattern, which is commonly observed in epithelioid hemangioendothelioma. However, the microscopic recognition of angiosarcoma arising in the endometrium may pose diagnostic problems, especially when the classic "freely anastomosing vascular channels" customarily described in better differentiated lesions are lacking or when the tumor is mainly composed of epithelioid or spindle cells with minimal features of endothelial derivation [3]. In these cases with endometrial mesenchymal tumors, immunohistochemical findings are helpful for excluding other diagnostic possibilities, including common ESS, in the diagnosis of rare uterine angiosarcoma. A small panel including multiple antibodies has been used for the diagnosis of uterine angiosarcomas in several reports (Table 1). Immunohistochemically, angiosarcomas express endothelial markers, such as CD31, CD34, and factor VIII [3,10,13,17]. In addition, lymphatic differentiation is common in angiosarcoma, and certain subsets are also positive for lymphatic endothelial markers, including D2-40 [9]. On the other hand, ESS is positive for CD10 and ER [2,12] and negative for endothelial markers, such as CD31 [1], CD34 [2], and factor VIII [1]. In our case, the tumor cells were diffusely positive for CD31 and D2-40 and were negative for CD10, ER, CD34, and factor VIII. These results are compatible with a classification of uterine angiosarcoma with lymphatic differentiation, according to the definition given in a previous report [4] (Table 1). The use of a small panel composed of CD10, ER, and CD34 is recommended for distinguishing tumors with a predominant hemangiopericytomatous growth pattern from ESS [2]. However, our case was immunohistochemically negative for CD10, ER, and CD34. The CD34 negativity, a definite marker for vascular differentiation, in the present case did not, by itself, provide solid support for our diagnosis. Instead, the addition of another panel that included D2-40 and CD31 was helpful for making a convincing diagnosis. Our experience suggests that a panel of markers including not only CD10, ER, and CD34, but also D2-40 and CD31 may be more helpful for a differential diagnosis of angiosarcomas from other tumors, including ESS.

The cause of angiosarcoma in the uterus, an uncommon location, remains largely speculative. Our case had concurrent leiomyomas in the myometrium, although the angiosarcoma in the endometrium was microscopically distant from the leiomyomas. In previous studies, two patients with uterine angiosarcomas also had concurrent uterine leiomyomas or leiomyomatosis, suggesting that increased vascular proliferation secondary to a mechanical pressure effect of adjacent leiomyomas might have induced the endothelial neoplastic transformation [3,13]. However, eight other cases of uterine angiosarcoma were not associated with uterine leiomyomas [3]. This finding suggests that whereas uterine angiosarcoma can arise in association with uterine leiomyomas, it commonly develops *de novo* [3,13]. However, little is known about the genetics of angiosarcomas.

On the other hand, the genes rearranged in t(10;17)(q22;p13), a recurrent aberration previously reported in a subset of clear cell sarcoma of the kidney in children [15], were recently identified in ESS [7]. This rearrangement results in an in-frame fusion between YWHAE (exons 1–5) and 1 of the 2 highly homologous genes FAM22A and FAM22B (exons 2–7), designated as YWHAE-FAM22 [7]. ESS carrying this fusion gene immunohistochemically exhibits cyclin D1 overexpression [6]. This gene rearrangement has never been observed in non-ESS tumors in adults [8,11]. In a very recent report, this fusion gene was not shown in 21 angiosarcomas of extrauterine soft tissue [8]. On the other hand, the tumor cells in our case were immunohistochemically positive for cyclin D1. Moreover, FISH analysis showed unpaired signals of FAM22A, FAM22B, and YWHAE locus, although it failed to identify the YWHAE-FAM22

Please cite this article in press as: S. Suzuki, et al., Breakages at YWHAE, FAM22A, and FAM22B loci in uterine angiosarcoma: A case report with immunohistochemical and genetic analysis, Pathol. – Res. Pract (2013), http://dx.doi.org/10.1016/j.prp.2013.09.009

Table 1
Summary of clinical and immunohistochemical results with a panel of antibodies in reported uterine angiosarcoma cases.

Authors [Ref.]	Age (years)	Symptoms	Tumor size	CD31	CD34	Factor VIII	D2-40
Schammel [17]	49	Pelvic mass and anemia	29.1 cm × 28.7 cm × 19 cm	(+)	(+)	(+)	ND
Schammel [17]	58	Vaginal bleeding and anemia	12 cm	(+)	(+)	(+)	ND
Schammel [17]	70	Vaginal bleeding	5.0 cm × 2.5 cm × 3.0 cm	(+)	(+)	(+)	ND
Schammel [17]	75	Vaginal bleeding	6.3 cm × 6.0 cm × 4.5 cm	(+)	(+)	(+)	ND
Mendez [10]	59	Pelvic mass and bleeding	12-week-size uterus	(+)	ND	(+)	ND
Cardinale [3]	81	Anemia	8 cm × 7 cm × 4.5 cm	(+)	(−)	(+)	(−)
Cardinale [3]	35	Shortness of breath, dry cough and gastrointestinal reflux	25 cm in larger dimension	(+)	(−)	(+)	(-)
Olawaiye [13]	54	Enlarged uterus on routine clinical examination	11 cm × 6 cm	(+)	(+)	ND	ND
Hayashi [4]	41	Abdominal distention, lower abdominal pain and vaginal bleeding	14 cm × 12 cm × 9 cm	(+)	(−)	(−)	(+)
Current case	62	Vaginal bleeding	3 cm in larger dimension	(+)	(−)	(−)	(+)

ND: not done.

fusion gene in tumor cells of our case by FISH and RT-PCR using formalin-fixed, paraffin-embedded tumor tissue [5]. These results suggested that a complicated situation including breakages of FAM22A, FAM22B, and YWHAE loci had been generated in the tumor cells in a manner similar to chromothripsis [18]. Breakages of these loci may play some common roles in the pathogenesis of two different uterine sarcomas: ESS and angiosarcoma.

Uterine angiosarcomas are highly aggressive neoplasms with extension beyond the uterus and recurrences that can occur within weeks to months of the initial diagnosis [3,13]. However, one reported case survived for 3 years after surgery alone; the lesion was 5 cm in size, polypoid, with invasion to one half of her myometrium, and the surgical resection margins were negative [17]. Our case also remained alive for 4 years after surgery without adjuvant therapy. A possible explanation for the extended survival in these two cases may be that in both cases, the tumor had invaded only half, and not the entire, thickness of the myometrium and the surgical resection margins were negative. Currently, the associations between breakages of loci including YWHAE and FAM22 and the prognosis or biological behavior of uterine angiosarcomas are uncertain. To address this issue, further studies are needed. In conclusion, we have described a case pertinent to the expansion of our knowledge regarding this rare uterine angiosarcoma, and the identification of YWHAE and FAM22 loci breakages in this tumor has provided new insights as to its pathogenesis.

Conflict of interest

The authors have no conflict of interest to declare.

Acknowledgments

We appreciate Ms. Kiyoko Nagura and Mr. Hisaki Igarashi for technical assistance. This case was presented at the Japanese Pathological Society Chubu Meeting on December 15, 2012, in Nagoya.

This contribution was supported, in part, by Grants-in-Aid for the U.S.-Japan Cooperative Medical Science Program; the National Cancer Center Research and Development Fund; Grant for priority areas from the Japanese Ministry of Education, Culture, Sports, Science and Technology [221S0001]; and Grants-in-Aid for Cancer Research from the Japanese Ministry of Health, Labour and Welfare [23120201 and 10103838], the Smoking Research Foundation, and the Princess Takamatsu Cancer Research Fund.

References

[1] V.M. Abeler, M. Nenodovic, Diagnostic immunohistochemistry in uterine sarcomas: a study of 397 cases, Int. J. Gynecol. Pathol. 30 (2011) 236–243.
[2] R. Bhargava, J. Shia, A.J. Hummer, H.T. Thaler, C. Tornos, R.A. Soslow, Distinction of endometrial stromal sarcomas from 'hemangiopericytomatous' tumors using a panel of immunohistochemical stains, Mod. Pathol. 18 (2005) 40–47.
[3] L. Cardinale, M. Mirra, C. Galli, J.R. Goldblum, S. Pizzolitto, G. Falconieri, Angiosarcoma of the uterus: report of 2 new cases with deviant clinicopathologic features and review of the literature, Ann. Diagn. Pathol. 12 (2008) 217–221.
[4] T. Hayashi, K. Koike, T. Kumasaka, T. Saito, K. Mitani, Y. Terao, D. Ogishima, T. Yao, S. Takeda, K. Takahashi, K. Seyama, Uterine angiosarcoma associated with lymphangioleiomyomatosis in a patient with tuberous sclerosis complex: an autopsy case report with immunohistochemical and genetic analysis, Hum. Pathol. 43 (2012) 1777–1784.
[5] A. Isphording, R.H. Ali, J. Irving, A. Goytain, N. Nelnyk, L.N. Hoang, C.B. Gilks, D.G. Huntsman, T.O. Nielsen, M.R. Nucci, C.H. Lee, YWHAE-FAM22 endometrial stromal sarcoma: diagnosis by reverse transcription-polymerase chain reaction in formalin-fixed, paraffin-embedded tumor, Hum. Pathol. 44 (2013) 837–843.
[6] C.H. Lee, R.H. Ali, M. Rouzbahman, A. Marino-Enriquez, M. Zhu, X. Guo, A.L. Brunner, S. Chiang, S. Leung, N. Nelnyk, D.G. Huntsman, C. Blake Gilks, T.O. Nielsen, P. Dal Cin, M. van de Rijn, E. Oliva, J.A. Fletcher, M.R. Nucci, Cyclin D1 as a diagnostic immunomarker for endometrial stromal sarcoma with YWHAE-FAM22 rearrangement, Am. J. Surg. Pathol. 36 (2012) 1562–1570.
[7] C.H. Lee, A. Marino-Enriquez, W. Ou, M. Zhu, R.H. Ali, S. Chiang, F. Amant, C.B. Gilks, M. van de Rijn, E. Oliva, M. Debiec-Rychter, P. Dal Cin, J.A. Fletcher, M.R. Nucci, The clinicopathologic features of YWHAE-FAM22 endometrial stromal sarcomas: a histologically high-grade and clinically aggressive tumor, Am. J. Surg. Pathol. 36 (2012) 641–653.
[8] C.H. Lee, W.B. Ou, A. Marino-Enriquez, M. Zhu, M. Mayeda, Y. Wang, X. Guo, A.L. Brunner, F. Amant, C.A. French, R.B. West, J.N. McAlpine, C.B. Gilks, M.B. Yaffe, L.M. Prentice, A. McPherson, S.J. Jones, M.A. Marra, S.P. Shah, M. van de Rijn, D.G. Huntsman, P. Dal Cin, M. Debiec-Rychter, M.R. Nucci, J.A. Fletcher, 14-3-3 fusion oncogenes in high-grade endometrial stromal sarcoma, Proc. Natl. Acad. Sci. U. S. A. 109 (2012) 929–934.
[9] C.C. Mankey, J.B. McHugh, D.G. Thomas, D.R. Lucas, Can lymphangiosarcoma be resurrected? A clinicopathological and immunohistochemical study of lymphatic differentiation in 49 angiosarcomas, Histopathology 56 (2010) 364–371.
[10] L.E. Mendez, S. Joy, R. Angioli, R. Estape, M. Penalver, Primary uterine angiosarcoma, Gynecol. Oncol. 75 (1999) 272–276.
[11] F. Mitelman, B. Johansson, F. Mertens, The impact of translocations and gene fusions on cancer causation, Nat. Rev. Cancer 7 (2007) 233–245.
[12] F. Moinfar, M. Azodi, F.A. Tavassoli, Uterine sarcomas, Pathology 39 (2007) 55–71.
[13] A.B. Olawaiye, J.A. Morgan, A. Goodman, A.F. Fuller Jr., R.T. Penson, Epithelioid angiosarcoma of the uterus: a review of management, Arch. Gynecol. Obstet. 278 (2008) 401–404.
[14] J.R. Prensner, A.M. Chinnaiyan, Oncogenic gene fusions in epithelial carcinomas, Curr. Opin. Genet. Dev. 19 (2009) 82–91.
[15] D. Rakheja, A.G. Weinberg, G.E. Tomlinson, K. Partridge, N.R. Schneider, Translocation (10;17)(q22;p13): a recurring translocation in clear cell sarcoma of kidney, Cancer Genet. Cytogenet. 154 (2004) 175–179.
[16] T. Sano, Y. Kitayama, H. Igarashi, M. Suzuki, F. Tanioka, K. Chida, K. Okudela, H. Sugimura, Chromosomal numerical abnormalities in early stage lung adenocarcinoma, Pathol. Int. 56 (2006) 117–125.
[17] D.P. Schammel, F.A. Tavassoli, Uterine angiosarcomas: a morphologic and immunohistochemical study of four cases, Am. J. Surg. Pathol. 22 (1998) 246–250.
[18] T. Shibata, Cancer genomics and pathology: all together now, Pathol. Int. 62 (2012) 647–659.
[19] H. Sugimura, Detection of chromosome changes in pathology archives: an application of microwave-assisted fluorescence *in situ* hybridization to human carcinogenesis studies, Carcinogenesis 29 (2008) 681–687.
[20] H. Sugimura, H. Mori, K. Nagura, S. Kiyose, H. Tao, M. Isozaki, H. Igarashi, K. Shinmura, A. Hasegawa, Y. Kitayama, F. Tanioka, Fluorescence *in situ* hybridization analysis with a tissue microarray: 'FISH and chips' analysis of pathology archives, Pathol. Int. 60 (2010) 543–550.
[21] K. Yoshida, M. Sanada, S. Ogawa, Deep sequencing in cancer research, Jpn. J. Clin. Oncol. 43 (2013) 110–115.

Please cite this article in press as: S. Suzuki, et al., Breakages at YWHAE, FAM22A, and FAM22B loci in uterine angiosarcoma: A case report with immunohistochemical and genetic analysis, Pathol. – Res. Pract (2013), http://dx.doi.org/10.1016/j.prp.2013.09.009

Pathology – Research and Practice 210 (2014) 383–388

Contents lists available at ScienceDirect

Pathology – Research and Practice

journal homepage: www.elsevier.com/locate/prp

Teaching cases

A rare Japanese case with a NUT midline carcinoma in the nasal cavity: A case report with immunohistochemical and genetic analyses

Shioto Suzuki[a,*], Nobuya Kurabe[b], Hiroshi Minato[c], Aki Ohkubo[d], Ippei Ohnishi[a], Fumihiko Tanioka[a], Haruhiko Sugimura[b]

[a] Division of Pathology, Iwata City Hospital, Japan
[b] Department of Tumor Pathology, Hamamatsu University School of Medicine, Japan
[c] Department of Pathology and Laboratory Medicine, Kanazawa Medical University, Japan
[d] Division of Otolaryngology, Iwata City Hospital, Japan

ARTICLE INFO

Article history:
Received 19 November 2013
Received in revised form 6 January 2014
Accepted 30 January 2014

Keywords:
NUT midline carcinoma
Nasal cavity
Japanese
t(15 ;19)

ABSTRACT

Background: NUT (nuclear protein in testis) midline carcinoma (NMC) is a recently described aggressive malignancy that is genetically defined by rearrangements of the *NUT* locus at 15q14. In approximately two-thirds of cases, the characteristic t(15;19) results in the fusion oncogene *BRD4-NUT*. Only 10 sinonasal NMCs have been documented, none of which were Japanese cases.
Case presentation: An 18-year-old woman was admitted because of a rapidly progressing tumor in the nasal cavity. A biopsy revealed an undifferentiated neoplasm without squamous differentiation. The tumor cells had round to oval nuclei with vesicular chromatin, prominent nucleoli, and scant cytoplasm. Immunohistochemical staining demonstrated a strong positivity for vimentin and NUT, with focal CD138 and only spotty EMA and cytokeratin AE1/AE3 staining. Cytogenetic and fluorescence in situ hybridization analyses revealed a t(15;19) and *BRD4-NUT* gene rearrangement. Direct sequencing identified the in-frame fusion of exon11 of *BRD4* with exon2 of *NUT*. The patient was transferred to another hospital for chemoradiotherapy.
Conclusion: We herein describe the first Japanese case with an NMC of the sinonasal cavity, providing detailed and unambiguous cyto- and molecular genetic information on *BRD4-NUT*-rearrangement. The accumulation of cases with well-documented genetic data should provide clues to the treatment of this tumor entity.

Introduction

Several malignant tumors of the sinonasal tract may present with an undifferentiated morphology [6,20]. Overall, these tumors pose significant diagnostic challenges to attending surgical pathologists, especially in cases in which a limited amount of biopsy material is available [6] and in cases that do not exhibit the typical immunohistochemical results [3]. Among these sinonasal malignant neoplasms, nuclear protein in testis (NUT) midline carcinoma (NMC) is a recently recognized entity that is characterized by a poor prognosis [1,20].

The current recognition of the NMC entity is genetically defined by rearrangements of the *NUT* locus at 15q14, resulting in a fusion transcript with a member of the bromodomain-containing protein (BRD) family, usually *BRD4* located on chromosome 19p13.1 [7,10]. As NMC is a recently described tumor entity, it is still unfamiliar to most pathologists [14,16,20]. The histological features of tumors that have been reported as NMCs range from entirely undifferentiated carcinomas to carcinomas with prominent squamous differentiation [2–4,10,19]. Thus, the diagnosis of NMC simply based on morphology is difficult. Until recently, only one molecular method within the realm of diagnostic pathology, i.e., fluorescence in situ hybridization (FISH), was available for the robust demonstration of a rearrangement of the *NUT* gene [3,8,19]. Consequently, this entity has been commonly undiagnosed or misdiagnosed in clinical pathology practice, and comprehensive information, such as the correlation between the molecular features and the biological behaviors of this cancer, is limited. Since the identification of a somatic rearrangement involving the *NUT* gene in NMC [7], only

* Corresponding author at: Division of Pathology, Iwata City Hospital, 512-3 Ookubo, Iwata, Shizuoka 438-8550, Japan. Tel.: +81 538 38 5000; fax: +81 538 38 5047.
E-mail address: shiosuzuki-path@umin.net (S. Suzuki).

http://dx.doi.org/10.1016/j.prp.2014.01.013
0344-0338/

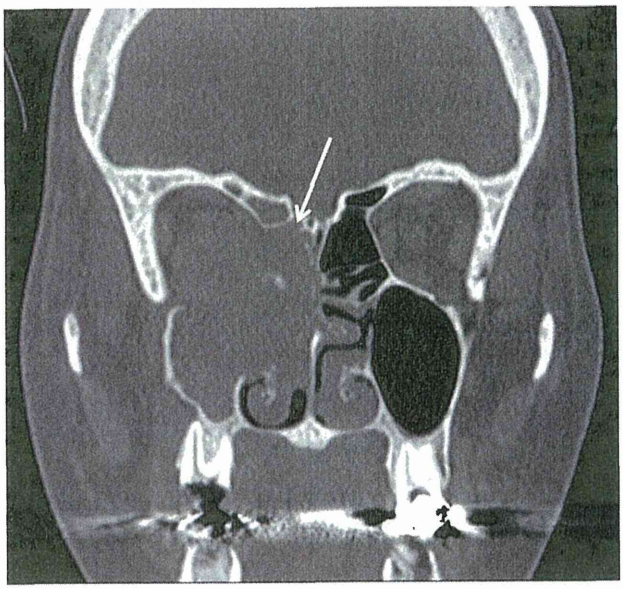

Fig. 1. CT scan of head obtained upon admission. The tumor occupies the right nasal cavity and maxillary and ethmoidal sinus, involving the ethmoid bone (arrow).

a few reports have determined the fusion gene in clinical specimens using a direct sequencing method [7,9,12,23]. NMCs are rare [1,10,20], and the geographic distribution of reported cases has been concentrated in the United States [1]. NMCs most often occur in the midline, including the head and neck, and the thorax [10,20]. Although the sinonasal tract is considered a preferential site in the head and neck region, only 10 sinonasal NMCs have been documented [2,3,8,13,19], none of which were Japanese cases.

In this article, we describe a new Japanese case with NMC in the nasal cavity; the NMC was diagnosed using immunohistochemistry with a highly sensitive and specific NUT monoclonal antibody [11]. In addition, a *BRD4-NUT* fusion gene, as the mechanism of NUT overexpression, was defined by karyotyping as well as molecular methods, including FISH and RT-PCR direct sequencing.

Clinical summary

An 18-year-old woman sought medical advice because of nasal discharge containing blood accompanied by pain with a 1-month duration. A computed tomography scan performed at the time of hospitalization revealed a mass in the right nasal cavity, and maxillary and ethmoidal sinus (Fig. 1). The mass involved the ethmoid bone (Fig. 1, arrow). A biopsy was performed.

Material and methods

Histopathologic and immunohistochemical examination

All the tissues were fixed in 10% buffered formalin and were embedded in paraffin after routine processing, followed by sectioning and staining with hematoxylin and eosin (H&E). Immunostaining was performed using antibodies for the following antigens: CD34 class II (DAKO, Glostrup, Denmark), CD45 (DAKO), CD56 (Leica Biosystems, Newcastle, United Kingdom), CD99 (DAKO), CD138/Syndecan-1 (DAKO), c-kit (DAKO), cytokeratin AE1/AE3 (DAKO), desmin (DAKO), epithelial membrane antigen (EMA, DAKO), hCG (DAKO), myogenin (DAKO), neuron-specific enolase (Nichirei, Tokyo, Japan), NUT (Cell Signaling Technologies Inc., Danvers, MA), PLAP (Leica Biosystems), S-100 (DAKO), and synaptophysin (DAKO).

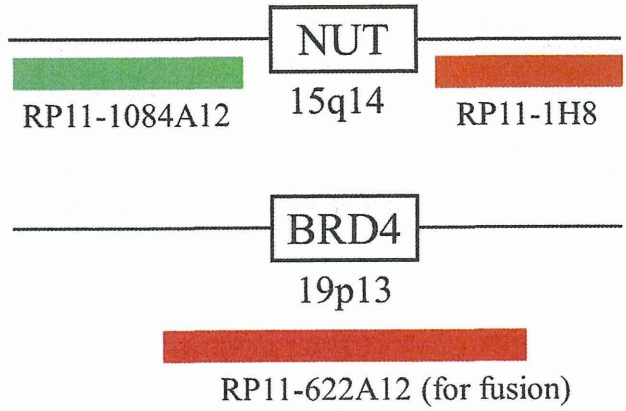

Fig. 2. Chromosomal positions of FISH probes flanking or including the genes of interest (*NUT* and *BRD4*).

FISH

The FISH procedure was performed as previously reported [21,22]. FISH probes were prepared from the Bacterial Artificial Chromosome (BAC) library. BAC probes flanking *NUT* (RP11-1084A12 and RP11-1H8) and a BAC probe containing *BRD4* (RP11-622A12) were purchased from Advanced GenoTechs Co. (Tsukuba, Japan) (Fig. 2). All the probes were confirmed to be correct by hybridizing them to a metaphase human chromosome spread (data not shown). To detect the break apart of NUT, the RP11-1084A12 probe was nick-translated using Green dUTP (2N32-50; Abbot, IL, USA) and the RP11-1H8 probe was nick-translated using Orange dUTP (2N33-50; Abbot). The combinations of RP11-1084A12, RP11-1H8, and RP11-622A12 were used to detect the fusion of *BRD4* and *NUT*. To detect the fusion, the RP11-622A12 probe was nick-translated using Orange dUTP (2N33-50), while both the RP11-1084A12 and the RP11-1H8 probes were nick-translated using Green dUTP (2N32-50). The nuclei were stained with 4,6-diamino-2-phenyl indole dihydrochloride (DAPI, Abbot). The slides were reviewed manually with at least 50 tumor nuclei evaluated for each case, and a cutoff of >30% nuclei showing a split or fused signal was considered positive for the rearrangement of the genes.

Direct sequencing

BRD4-NUT fusion cDNA was amplified using PCR with Phusion (New England BioLabs, Beverly, MA, USA); direct sequencing was then performed as described previously [7]. The primers BR2276F (AAGTTGATGTGATTGCCGGCTCCTC) and *NUT*1194R (GAGGTCTCTGGGCTTTACGCTGACG) were used [7]. Gel-purified PCR products were cycle-sequenced by the incorporation of ABI PRISM Big Dye Terminators (Perkin-Elmer, Inc., Wellesley, MA) and analyzed using an ABI 3130 sequencer (Life Science Technologies, Carlsbad, CA, USA).

Pathological findings

The small amount of biopsy material that was obtained revealed an undifferentiated neoplasm with necrosis (Fig. 3a). The tumor cells had round to oval nuclei with vesicular chromatin, prominent nucleoli, and scant cytoplasm (Fig. 3b). Frequent mitotic figures (10/5 hpf) were observed (Fig. 3b, arrow). Squamous differentiation was not identified.

Immunohistochemical staining demonstrated a strong vimentin positivity (Fig. 4a) with focal CD138 (Fig. 4b) and only spotty EMA (Fig. 4c) and cytokeratin AE1/AE3 positivity. Negative staining